CHAPTER 10

NUMERICAL SIMULATION OF NONLINEAR WAVE TRANSFORMATION OVER A SUBMERGED PLATE

Xiping Yu * Masahiko Isobe † Akira Watanabe ‡

Abstract

The Euler equation of fluid motion is integrated in the vertical direction by assuming a hyperbolic cosine distribution of pressure, As a result, quasi-linear hyperbolic equations governing the wave motion above a solid bed are obtained. The equations are then applied to describing the wave transformation over a submerged plate.

An algorithm based on the method of characteristics is developed in the numerical computation. The wave reflection and transmission coefficients computed under various conditions are compared with the experimental data, and the overall agreement is found to be fairly satisfactory.

1 INTRODUCTION

Persistent efforts have been devoted to developing efficient and economical breakwaters. The efforts are still needed since new requirements are constantly brought up in the course of further developing coastal zones. As construction sites advanced offshore further and further and the water depth to be dealt with becomes larger and larger, fundamental changes take place even in the design concept of breakwaters. Among many initiatives, it is found that some simple structures are very promising to lower the design wave height for main structures and thus to achieve an overall optimum of the project concerned, or even to stand alone to create a relatively calm area. A submerged horizontal or slightly inclined plate represents one example of such new simple types of breakwaters.

*Graduate student, Dept. of Civil Eng., Univ. of Tokyo, Bunkyo-ku, Tokyo 113, Japan.

†Dr. Eng., Assoc. Prof., ditto.

‡Dr. Eng., Prof., ditto.

When incident waves propagate over a submerged plate, part of the wave energy is reflected because of the interaction between the flows above and below the plate. Under certain conditions waves even break above the plate and the energy is thus considerably dissipated. It is by virtue of the reflection and dissipation that a submerged plate functions as a breakwater. However, unlike conventional breakwater, the effectiveness of the submerged plate is very sensitive to the incident wave conditions as well as the dimensions and the placement of the plate. Proper design of the submerged plate breakwaters requires reliable evaluation of the wave reflection and energy dissipation as well as the associated wave transmission under various conditions.

The wave deformation due to a plate has been treated in several previous studies. For example, analytical solution has been obtained for horizontal plate under long wave condition (Hattori and Matsumoto, 1977), and a numerical model based on the time-dependent mild slope equation is also available (Aoyama et al., 1988).

Most of the previous studies are based on the linear wave theory. To ensure the effectiveness, however, the submerged depth of the plate should not be too large, and then the wave nonlinearity becomes significant over the plate. Furthermore, wave breaking, a typical nonlinear phenomenon, is necessary to serve as an energy dissipator to minimize the wave transmission and reflection. Simulation of nonlinear waves is thus needed. In the present study a set of wave equations including nonlinear terms is derived to describe the wave deformation over a submerged plate. The nonlinear equations are solved numerically by the method of finite characteristics. Numerical results are compared with experimental data.

2 GOVERNING EQUATION OF WAVE MOTION

Wave motion is fundamentally governed by the following continuity equation and Euler equations.

$$\frac{\partial u_j}{\partial x_j} + \frac{\partial w}{\partial z} = 0 \tag{1}$$

$$\frac{\partial u_i}{\partial t} + \frac{\partial}{\partial x_j}(u_i u_j) + \frac{\partial}{\partial z}(u_i w) + \frac{\partial}{\partial x_i}(\frac{p}{\rho}) = 0 \tag{2}$$

$$\frac{\partial w}{\partial t} + \frac{\partial}{\partial x_j}(w u_j) + \frac{\partial}{\partial z}(w w) + \frac{\partial}{\partial z}(\frac{p}{\rho}) + g = 0 \tag{3}$$

where, u_j ($j = 1,2$) and w are, respectively, the horizontal and vertical components of the velocity, p the pressure, ρ the fluid density, g the gravitational acceleration, x_j and z the horizontal and vertical coordinates, and t the time. Through denoting the water surface elevation by η and the still water depth by h, the kinematic boundary conditions on the free surface as well as at the solid bottom are expressed by

$$\frac{\partial \eta}{\partial t} + u_j^f \frac{\partial \eta}{\partial x_j} - w^f = 0 \tag{4}$$

$$u_j^b \frac{\partial h}{\partial x_j} + w^b = 0 \tag{5}$$

in which the superscript f and b represent the values at free surface and bottom, respectively.

It is known that the small amplitude wave theory gives the pressure as

$$\frac{p}{\rho} = -gz + g\eta \frac{\cosh k_{\mathrm{M}}(h+z)}{\cosh k_{\mathrm{M}}(h+\eta)} \tag{6}$$

where a modification has been made to assure that the pressure becomes exactly zero on the free surface, which does not violate the small amplitude assumption. The quantity k_{M} in Eq. (6) is the modified wave number determined by the following modified dispersion relation:

$$C_{\mathrm{M}}^2 = \frac{g}{k_{\mathrm{M}}} \tanh k_{\mathrm{M}}(h+\eta) \tag{7}$$

in which $C_{\mathrm{M}} = \sigma / k_{\mathrm{M}}$ is the modified wave celerity, and σ the angular frequency.

It has been shown that the small amplitude wave theory is adequate up to the location near the breaking point (e.g., Isobe, 1985). Hence Eq. (6) is regarded as valid in the shoaling zone. In the surf zone, while the small amplitude wave theory is no longer valid, the assumption of hydrostatic pressure distribution may be acceptable. Since Eq. (6) yields the hydrostatic pressure distribution when the water depth becomes small, it may still be a rather good approximation at this situation. Thus Eq. (6) is not erroneous except for a narrow region around the breaking point.

With the assumption of the pressure distribution expressed by Eq. (6), Eqs. (1) and (2) can be integrated with respect to z from the bottom ($z = -h$) to the free surface ($z = \eta$). By recognizing that η is a function of x_j and t, and h a function of x_j only, and introducing the boundary conditions (4) and (5), the continuity equation (1) is integrated as

$$\frac{\partial \eta}{\partial t} + \frac{\partial q_j}{\partial x_j} = 0 \tag{8}$$

where, $q_j = \int_{-h}^{\eta} u_j dz$ is defined as the component of fluid discharge in x_j direction. In a similar way, the integrated momentum equation (9) can be obtained by further considering that the pressure on the free surface vanishes.

$$\frac{\partial q_i}{\partial t} + \frac{\partial}{\partial x_j}\left(\beta \frac{q_i q_j}{h+\eta}\right) + \frac{\partial}{\partial x_i}(C_{\mathrm{M}}^2 \eta) - g\eta \frac{\partial \eta}{\partial x_i} - \frac{g\eta}{\cosh k_{\mathrm{M}}(h+\eta)} \frac{\partial h}{\partial x_i} = 0 \tag{9}$$

where β is the momentum factor. By assuming the vertical distribution of u_i as:

$$u_i = u_i^b(x_j, t) \cosh k_{\mathrm{M}}(h + z) \tag{10}$$

β can be derived as

$$\beta = n_{\mathrm{M}} \alpha \tag{11}$$

with

$$\alpha = \frac{g(h + \eta)}{C_{\mathrm{M}}^2} \tag{12}$$

$$n_{\mathrm{M}} = \frac{1}{2}[1 + \frac{2k_{\mathrm{M}}(h + \eta)}{\sinh 2k_{\mathrm{M}}(h + \eta)}] \tag{13}$$

Equations (8) and (9) govern the wave motion over a solid bottom. The equations are mathematically termed as quasi-linear hyperbolic differential equations, which have been extensively studied (Courant and Hilbert, 1962). Among many of the properties discovered, it is recognized that discontinuities are included in the solutions under certain conditions even if the initial and boundary conditions are continuous functions. The discontinuity is related to the breaking in wave dynamics (Stoker, 1957).

Since Eq. (9) is derived from the basic equations of ideal fluid flow, the momentum loss is neglected. When waves propagate into the surf zone, the energy loss due to nonlinearity may become remarkable. However, the mechanical energy loss does not always mean a noticeable momentum loss. In some cases, the energy loss is significant but the momentum loss may be negligible, as stated in many textbooks about hydraulic jump (e.g., Rouse, 1946). In the present study we use Eq. (9) and neglect the momentum loss.

Since the pressure distribution given by Eq. (6) is assumed, only progressive waves are considered. Complete or partial standing waves, which are the superposition of two wave trains propagating in the opposite directions, can also be dealt with. However, if there are some rapid changes in boundary conditions, which may cause scattering waves, the validity of Eq. (9) should be reexamined.

3 FORMULATION OF WAVE MOTION OVER SUBMERGED PLATE

3.1 Basic equations

In the following we deal with a vertically two-dimensional wave field in the x–z plane. As shown in Figure 1, the flow field is divided into the four regions: (i) the offshore

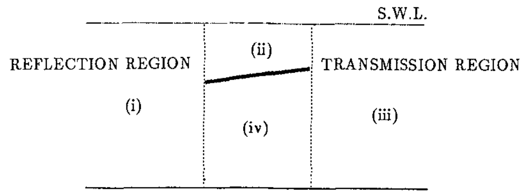

Figure 1: Definition sketch of submerged plate

or reflection region, (ii) the region above the plate, (iii) the onshore or transmission region, and (iv) the region under the plate. The flow in the regions (i), (ii) and (iii) can be described by the one-dimensional form of Eqs. (8) and (9).

In order to simplify the equations, we assume that the bottom slope is mild as

$$\left|\frac{\partial h}{\partial x}\right| \ll \left|\frac{\partial \eta}{\partial x}\right| \tag{14}$$

Furthermore, we neglect the terms originating from the nonlinearity but vanishing when the water depth becomes small, because the nonlinearity is considered to become significant only when the water depth is small. Then Eqs. (8) and (9) reduce to

$$\frac{\partial \eta}{\partial t} + \frac{\partial q}{\partial x} = 0 \tag{15}$$

$$\frac{\partial q}{\partial t} + 2\beta v \frac{\partial q}{\partial x} + (C_{\mathrm{M}}^2 - \beta v^2)\frac{\partial \eta}{\partial x} = 0 \tag{16}$$

where $v = q/(h+\eta)$ is the sectional mean velocity.

To derive the equation governing the flow under the plate, the procedure for deriving Eqs. (8) and (9) is followed. If the slope of the plate is small enough, it is expected that the hydrostatic pressure distribution may be assumed in the region (iv) because the flow can reasonably be treated as nearly parallel. Hence,

$$\frac{p}{\rho} = \frac{P_d}{\rho(h-d)} - gz \tag{17}$$

where P_d is the total dynamic pressure force on a vertical cross section below the plate, h and d are the total water depth and the depth above the plate, respectively. Eqs. (1), (2) and (5) are still valid, whereas the boundary condition on the plate becomes

$$u^p \frac{\partial d}{\partial x} + w^p = 0 \tag{18}$$

where the superscript p denotes the values on the surface of the plate. Substituting Eq. (17) into Eq. (2) and then integrating Eqs. (1) and (2) from $z=-h$ to $z=-d$ under the boundary conditions (5) and (18), we have

$$q = \text{const.} \tag{19}$$

$$\frac{\partial q}{\partial t} + \frac{\partial}{\partial x}\left(\frac{q^2}{h-d}\right) + \frac{\partial P_d}{\partial x} = 0 \tag{20}$$

Since q is only a function of t, Eq. (20) can be integrated with respect to x from one end of the plate to the other. Therefore, the differential equation for the fluid discharge under the plate is finally given as:

$$\frac{\partial q}{\partial t} + q^2 \frac{\tan\theta}{(h-d_d)(h-d_u)} + \frac{P_{dd}-P_{du}}{l\cos\theta} = 0 \tag{21}$$

where l and θ are the length and slope angle of the plate and the subscript u and d represent the values at the upstream and downstream ends of the plate, respectively.

3.2 Boundary Conditions

At the offshore lateral boundary of the reflection region (i), waves are assumed to be described by the superposition of the incident and reflected waves as

$$\eta = \eta_{\mathrm{I}}(x - C_h t) + \eta_{\mathrm{R}}(x + C_h t) \tag{22}$$

where the subscripts I and R represent, respectively, the incident and reflected waves; C_h is the wave celerity in the region of constant water depth h. By differentiating η with respect to t and x, it is found that

$$\frac{\partial \eta}{\partial t} - C_h \frac{\partial \eta}{\partial x} = 2\frac{\partial \eta_{\mathrm{I}}}{\partial t} \tag{23}$$

Equation (23) gives the offshore lateral boundary condition. In a similar way, at the onshore lateral boundary of the region (iii), it can be assumed that

$$\eta = \eta_{\mathrm{T}}(x - C_h t) \tag{24}$$

where the subscript T represents the transmitted waves. The onshore lateral boundary condition can thus be obtained as:

$$\frac{\partial \eta}{\partial t} + C_h \frac{\partial \eta}{\partial x} = 0 \tag{25}$$

Generally, under the boundary conditions periodic in time, a solution of hyperbolic differential equation consists of two parts: one is the contribution of the boundary conditions and thus also periodic; the other is the contribution of the initial condition which decays rapidly with time if any damping factor is included. In many practical problems of coastal engineering, only the periodic solution is important. As a result, it allows the initial conditions to be arbitrarily specified so far as they will become trivial after several wave period. In the present case, however, the boundary conditions are given in terms of differential equations. Hence, arbitrary constants involved should be determined so as to make the solution unique. Since the constants may implicitly be specified in the initial conditions of q and η, there should be certain restriction on the specification of q and η at the initial step. However, the state of still water can be utilized as reasonable initial conditions if we do not consider any steady current.

The matching boundary conditions at both ends of the plate are

$$\eta_h = \eta_a \tag{26}$$

$$q_h = q_a + q_b \tag{27}$$

$$\frac{P_{db}}{\rho} = \frac{P_{dh} - P_{da}}{\rho} \tag{28}$$

where the subscripts h, a and b represent, respectively, the values at the region of constant water depth, above and below the plate. It is obvious that Eqs. (26), (27) and (28) physically imply the continuity of the free surface, the conservation of mass and the balance of the pressure force. The substitution of Eq. (6) into Eq. (28) gives

$$\frac{P_{db}}{\rho} = (C_{\mathrm{M}h}^2 - C_{\mathrm{M}a}^2)\eta_h \tag{29}$$

4 METHOD OF FINITE CHARACTERISTICS

The method of characteristics has been developed as an effective technique to solve quasi-linear hyperbolic differential equations. By introducing two families of characteristic curves in the x-t plane, partial differential equations are replaced by the characteristic equations including only ordinary derivatives along the characteristic curves.

Equations (15) and (16) can be rewritten in a matrix form as:

$$\frac{\partial}{\partial t}\begin{pmatrix} \eta \\ q \end{pmatrix} + \begin{bmatrix} 0 & 1 \\ C_{\mathrm{M}}^2 - \beta v^2 & 2\beta v \end{bmatrix} \frac{\partial}{\partial x}\begin{pmatrix} \eta \\ q \end{pmatrix} = 0 \tag{30}$$

It has been shown that the slopes of the characteristic curves are equal to the two eigenvalues of the coefficient matrix (Abbott, 1979). Thus,

$$\begin{aligned}\frac{dx}{dt} &= \beta v \pm \sqrt{\beta(\beta-1)v^2 + C_{\mathrm{M}}^2} \\ &\equiv \xi_{\pm}\end{aligned} \tag{31}$$

The characteristic equations are, then

$$\frac{dq}{dt} - \xi_{\mp}\frac{d\eta}{dt} = 0 \tag{32}$$

Several numerical techniques for solving the characteristic equations are available (Lin, 1952; Freemman and LeMehaute, 1964; Abbott and Verwey, 1970). Here a scheme, called the method of finite characteristics, is introduced through the improvement of Lin's method. The improvement, which is to include some higher order terms in the computation, has been found necessary because the ratio of the grid size to the wavelength in the computation of sea waves can not be as small as that for flood waves, owing to the restriction of the computational time.

The method of finite characteristics can be explained by Figure 2. Two finite charac-

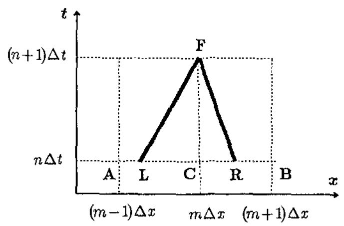

Figure 2: Definition sketch for FCM

teristic curves are issued backward from the computation point F toward the previous time step. The finite characteristic curves are approximated by straight lines with the slope determined through the algorithmic form of Eq. (31)

$$x_F - x_L = \xi_{+,L}\Delta t \tag{33}$$

$$x_F - x_R = \xi_{-,R}\Delta t \tag{34}$$

where the subscripts F, L and R express the values at the points F, L and R. $\xi_{+,L}$ and $\xi_{-,R}$ are computed through linear interpolation of the values at the grid points A, B and C as follows:

$$\xi_{+,L} = \xi_{+,C} - \frac{x_L - x_C}{\Delta x}(\xi_{+,A} - \xi_{+,C}) \tag{35}$$

$$\xi_{-,R} = \xi_{-,C} + \frac{x_R - x_C}{\Delta x}(\xi_{-,B} - \xi_{-,C}) \tag{36}$$

By substituting Eqs. (35) and (36) into Eqs. (33) and (34), the positions x_L and x_R are explicitly expressed as:

$$x_L = x_F - \frac{\xi_{+,C}\Delta t}{1 + \frac{\Delta t}{\Delta x}(\xi_{+,C} - \xi_{+,A})} \tag{37}$$

$$x_R = x_F - \frac{\xi_{-,C}\Delta t}{1 + \frac{\Delta t}{\Delta x}(\xi_{-,B} - \xi_{-,C})} \tag{38}$$

Provided that the positions of the points L and R are determined, the values of η and q at these points are computed through the following second order interpolation.

$$\begin{aligned} \begin{pmatrix} \eta \\ q \\ \xi_\pm \end{pmatrix}_{L;R} &= \begin{pmatrix} \eta \\ q \\ \xi_\pm \end{pmatrix}_A \frac{(x_{L;R} - x_C)(x_{L;R} - x_B)}{2\Delta x^2} \\ &- \begin{pmatrix} \eta \\ q \\ \xi_\pm \end{pmatrix}_B \frac{(x_{L;R} - x_A)(x_{L;R} - x_B)}{\Delta x^2} \\ &+ \begin{pmatrix} \eta \\ q \\ \xi_\pm \end{pmatrix}_C \frac{(x_{L;R} - x_A)(x_{L;R} - x_C)}{2\Delta x^2} \end{aligned} \tag{39}$$

On the other hand, Eq. (32) is discretized along the finite characteristic curves as

$$q_F - q_L = \xi_{-,L}(\eta_F - \eta_L) \tag{40}$$

$$q_F - q_R = \xi_{+,R}(\eta_F - \eta_R) \tag{41}$$

Hence, η_F and q_F can be expressed in terms of η_L, η_R, q_L, q_R, $\xi_{-,L}$ and $\xi_{+,R}$ as:

$$\eta_F = \frac{\xi_{-,L}\eta_L - \xi_{+,R}\eta_R - (q_L - q_R)}{\xi_{-,L} - \xi_{+,R}} \tag{42}$$

$$q_F = \frac{\xi_{-,L}q_R - \xi_{+,R}q_R + \xi_{-L}\xi_{+,R}(\eta_L - \eta_R)}{\xi_{-,L} - \xi_{+,R}} \tag{43}$$

When the computational point is located at the matching boundaries, the discontinuity of q should be considered. The jump of the value of q is determined through the matching boundary condition (27) as well as the algorithmic form of Eq. (21), that is

$$q^{n+1} = q^n - [q^{n+1}q^n \frac{\tan\theta}{(h - d_d)(h - d_u)} + \frac{P_{dd}^n - P_{du}^n}{l\cos\theta}]\Delta t \tag{44}$$

The offshore and onshore boundary conditions are discretized as:

$$\eta_{\text{off}}^{n+1} = \eta_{\text{off}}^{n} + [C_h \frac{\partial \eta}{\partial x}\Big|_{\text{off}}^{n} + 2\frac{\partial \eta_{\text{I}}}{\partial t}\Big|^{n}]\Delta t \tag{45}$$

$$\eta_{\text{on}}^{n+1} = \eta_{\text{on}}^{n} - C_h \frac{\partial \eta}{\partial x}\Big|_{\text{on}}^{n} \Delta t \tag{46}$$

in which $\partial\eta/\partial x\Big|_{\text{off}}^{n}$ and $\partial\eta/\partial x\Big|_{\text{on}}^{n}$ are calculated through the numerical differentiation method based on Lagrangian interpolation formula (Hildebrand, 1987).

Lin's method was initially developed for the computation of continuous flow, but its further application have shown that it can also simulate discontinuities (Lin et al., 1982).

As long as the water surface elevation near the lateral boundaries is obtained, the reflection coefficient K_{R} and the transmission coefficient K_{T} can easily be calculated.

5 SOME COMPUTATIONAL RESULTS

Wave reflection and transmission coefficients are dependent on the incident wave conditions as well as the placement of the plate. The incident wave steepness H_{I}/L_0, the relative water depth h/L_0, the relative submerged depth d/h, the slope of the plate $\tan\theta$ and the relative length of the plate l/L_0 can be chosen as independent dimensionless parameters. To investigate the relationships, the variation of K_{R} and K_{T} against l/L_0 is computed for various values of the other parameters. The results are shown in Figs. 3 to 6 along with the experimental data. Table 1 summarizes the conditions.

Figure 3 shows the comparison of reflection and transmission coefficients among linear waves and waves with different incident steepness. It can be found that the influence of the incident wave steepness becomes remarkable when the wave nonlinearity is considered; the transmission coefficient decreases with the increase of the incident wave steepness.

Figure 4 shows the change in the wave reflection and transmission coefficients against the submerged depth of the plate. Since wave motion decays downwards from the free surface, too large a submerged depth of the plate makes little contribution to the wave deformation.

Figure 5 shows the variation of the reflection and transmission coefficients of waves with different relative water depth. It is found that for a given relative length of the plate, the reflection and transmission coefficients does not show very large difference for the wide change of the relative water depth. This indicates, as naturally expected,

Table 1: Conditions for computation and experiment

CASE		h(cm)	T(s)	H_I(cm)	d/h	$\tan\theta$
	1	20.0	0.80	SMALL	0.2	0.0
	2	20.0	0.80	1.5	0.2	0.0
STP	3	20.0	0.80	3.6	0.2	0.0
	1	20.0	0.80	2.0	0.2	0.0
SMD	2	20.0	0.80	2.0	0.5	0.0
	1	20.0	0.88	1.5	0.2	0.0
RWD	2	20.0	0.62	2.0	0.2	0.0
	1	20.0	0.80	1.8	0.3	0.2
SLP	2	20.0	0.80	1.8	0.3	0.4

that for a given absolute length of the plate, longer waves are easier to transmit over the plate. For very long waves, like tsunami, a plate can not function at all as a breakwater.

Figures 6 indicates that there is no significant change in the reflection and transmission coefficients with the slope of the plate if the mean submerged depth is kept constant. The computation for the inclined plate is available only for l/L_0 less than a certain value, because a longer plate would emerge from the free surface, for which the present model is not valid.

6 CONCLUDING REMARKS

A mathematical model of nonlinear wave motion has been developed and applied to simulating the wave transformation over a submerged plate. Numerical computation based on the method of finite characteristics for general conditions have been proposed. The computed wave reflection and transmission coefficients have been compared with the experimental data under various conditions. The overall agreement is satisfactory.

References

[1] Abbott, M. B., 1979: *Computational Hydraulics*, The Pitman Press, 324p.

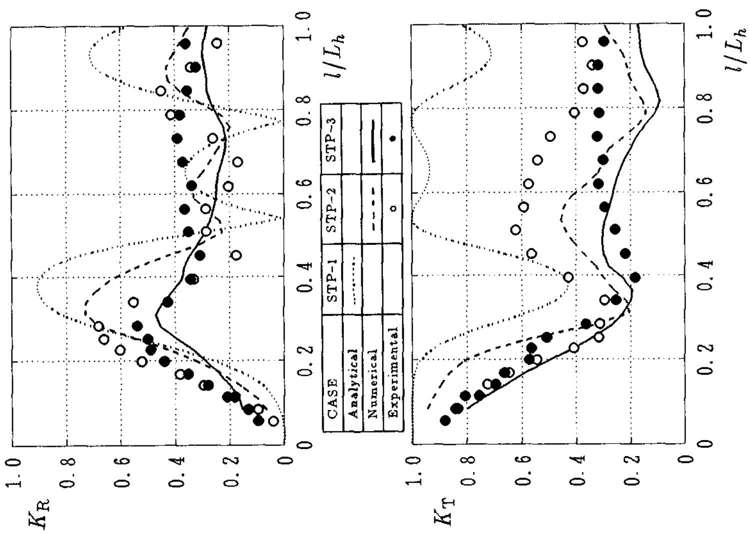

Figure 3 Computed and measured K_R and K_T (case STP)

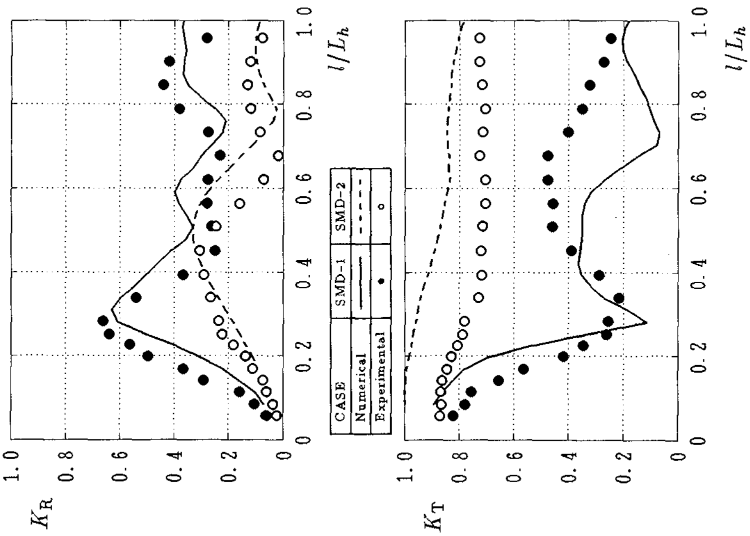

Figure 4 Computed and measured K_R and K_T (case SMD)

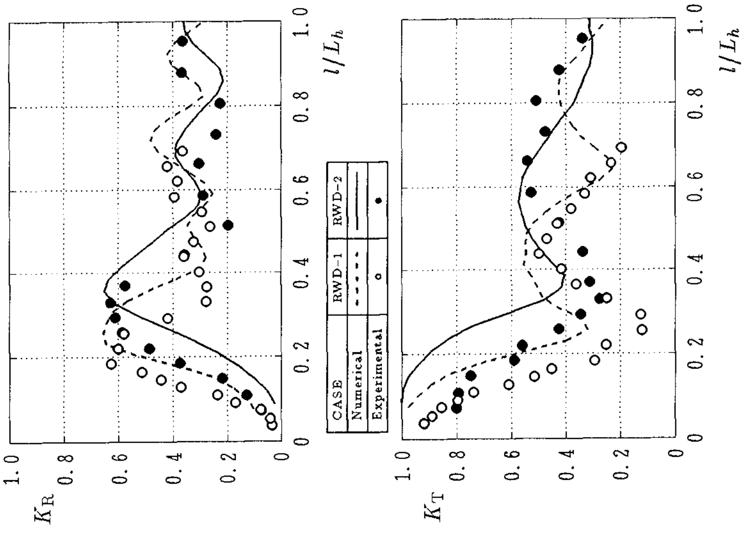

Figure 5 Computed and measured K_R and K_T (case RWD)

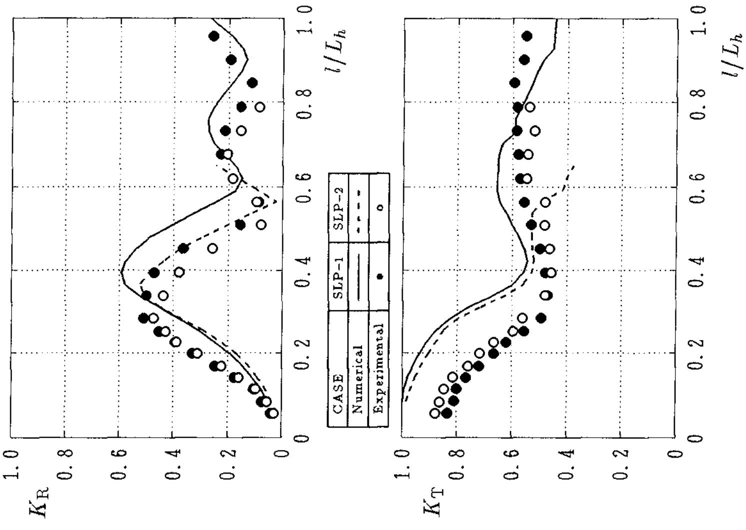

Figure 6 Computed and measured K_R and K_T (case SLP)

[2] Abbott, M. B. and A. Verwey, 1970: Four-point method of characteristics, *J. of the hydraulics division*, ASCE, Vol. 96, No. HY12, pp. 2549–2564.

[3] Aoyama, T., M. Isobe, T. Izumiya and A. Watanabe, 1988: Study on wave control in offshore region using a submerged plate, *35th Japanese Conf. on Coastal Eng.*, pp. 507–511 (in Japanese).

[4] Courant, R. and D. Hilbert, 1962: *Method of Mathematical Physics*, Vol.2, Interscience Publisher, 839p.

[5] Freeman, J. C. and B. LeMehaute, 1964: Wave breaks on a beach slope and surges on a dry bed, *J.of the Hydraulics division*, ASCE, Vol. 90, No. HY2, pp. 187–216.

[6] Hattori, M. and H. Matsumoto, 1977: Hydraulic performances of a submerged horizontal plate breakwater, *24th Japanese Conf. on Coastal Eng.*, pp. 266–270 (in Japanese).

[7] Hildebrand, F. B., 1974: *Introduction to Numerical Analysis*, Dover publications, 669p.

[8] Isobe, M., 1985: Calculation and application of first order cnoidal wave theory, *Coastal Eng.*, Vol. 9, pp. 309–325.

[9] Lin, P. N., 1952: Numerical analysis of continuous unsteady flow in open channel, *Trans. Amer. Geophys. Union*, Vol. 33, No. 2, pp. 226–234.

[10] Lin, B., Z. Dai and K. Li, 1982: Unsteady flow studies in China, *J. Waterway Port Coastal and Ocean Division.*, ASCE, Vol. 108, No. WW3, pp. 343–360.

[11] Rouse, H., 1964: *Elementary Mechanics of Fluids*, Dover Publication, 376p.

[12] Stoker, J. J., 1957: *Water Waves*, Interscience, 567p.